Hindawi
Modelling and Simulation in Engineering
Volume 2019, Article ID 7878564, 16 pages
https://doi.org/10.1155/2019/7878564

Research Article

Nonlinear Transient Thermal Modeling and Analysis of a Convective-Radiative Fin with Functionally Graded Material in a Magnetic Environment

M. G. Sobamowo,[1] **G. A. Oguntala**,[2] **and A. A. Yinusa**[1]

[1]*Department of Mechanical Engineering, University of Lagos, Akoka, Lagos State, Nigeria*
[2]*School of Electrical Engineering and Computer Science, Faculty of Engineering and Informatics, University of Bradford, West Yorkshire, UK*

Correspondence should be addressed to M. G. Sobamowo; mikegbeminiyi@gmail.com

Received 21 August 2018; Revised 20 December 2018; Accepted 23 December 2018; Published 14 February 2019

Academic Editor: Farouk Yalaoui

Nonlinear transient thermal analysis of a convective-radiative fin with functionally graded materials (FGMs) under the influence of magnetic field is presented in this study. The developed nonlinear thermal models of linear, quadratic, and exponential variation of thermal conductivity are solved approximately and analytically using the differential transformation method (DTM). In order to verify the accuracies of the nonlinear solutions, exact analytical solutions are also developed with the aids of Bessel, Legendre, and modified Bessel functions. Good agreements are established between the exact and the approximate analytical solutions. In the parametric studies, effects of heat enhancement capacity of fin with functionally graded material as compared to fin with homogeneous material are investigated. Also, influence of the Lorentz force and radiative heat transfer on the thermal performance of the fin are analyzed. From the results, it is shown that increase in radiative and magnetic field parameters as well as the in-homogeneity index improve the thermal performance of the fin. Also, the transient responses reveal that the FGM fin with quadratic-law and exponential-law function shows the slowest and fasted thermal responses, respectively. This study will provide a very good platform for the design and optimization of an improved heat transfer enhancement in thermal systems, where the surrounding fluid is influenced by a magnetic field.

1. Introduction

The increasing demands for high-performance engineering systems come with inherent increased heat generation in the thermal and electronics systems which consequently lead to increased thermal damages. Effective thermal management and dissipation of excess heat from heat transfer components have been a major concern and challenge in the design of the thermal and electronic systems. In the quest for the thermal management of these systems, the heat sink has proved to be an effective, passive means of reducing the thermally induced failures by enhancing heat dissipation from thermal systems and electronics systems. Heat sinks are heat exchangers used in dissipating heat from functional thermal systems to the environment to ensure whether the device operates within safe temperature limits. The wide range of applications of heat sinks in cooling different electronic and micro electronics components such as the central processing unit (CPU), high-power semiconductor devices, high-power lasers, light-emitting diodes (LEDs), and sensitive devices affirm its effectiveness as a passive mode of cooling of thermal systems. The improvement of the thermal performance of heat sink and consequently energy saving in the thermal system is timely owing to miniaturization in size of thermal systems, acoustic control due to its destructive effects, and energy saving using smaller fan size.

To improve the thermal performance of cooling devices using porous fin as a passive method for heat transfer enhancement in thermal equipment, different authors have proposed different innovative analysis and approach, succeeding the pioneer of work of Kiwan and Al-Nimr [1] and Kiwan [2–4] on the thermal performance analysis of porous fin in the natural convection environment. Shalchi-Tabrizi and Seyf [5] employed nanofluid and presented the entropy generation and convective heat transfer in a micro heat sink. Hashemi et al. [6] investigated the heat transfer enhancement in a miniature heat sink using nanofluid, while Hung et al. [7] presented a study on heat transfer enhancement in micro channel heat sinks using nanofluids. Seyf and Feizbakhshi [8] carried out a computational analysis of nanofluid effects on convective heat transfer enhancement of micro pin fin heat sinks, while Fazeli et al. [9] investigated experimentally and numerically the heat transfer in a miniature heat sink utilizing silica nanofluid. However, other studies focus on the properties of conventional airflow and features of channel cross section as an approach to improve heat transfer enhancement in heat sinks. In these studies, Kim and Mudawar [10] developed analytical heat diffusion models for different micro channel heat sink cross-sectional geometries. Naphon et al. [11] presented a numerical investigation of the heat transfer flow in the minifin heat sink for CPU. Naphon and Khonseur [12] studied the convective heat transfer and pressure drop in the micro channel heat sink whilst Kim and Kim [13] investigated fluid flow and the characteristics of heat transfer in cross-cut heat sinks. Furthermore, the effects of various geometries and airflow paths on the heat sink performance have also been investigated in the previous literature. Hung et al. [14] analyzed the heat transfer characteristics of the double-layered micro channel heat sink. Wan et al. [15] presented an experimental analysis of flow and heat transfer in a miniature porous heat sink for high heat flux applications. Lelea [16] studied the effects of inlet geometry on heat transfer and fluid flow of tangential micro heat sink. Yu et al. [17] presented an enhanced heat transfer study using a plate-pin fin heat sink. Chai et al. [18] carried out a numerical simulation of fluid flow and heat transfer in a micro channel heat sink with offset fan-shaped reentrant cavities in sidewall. The previous studies explored the convective parameters around the heat sink while some past research works employed the properties of the conventional airflow, features of channel cross section, variable geometries, and airflow paths to enhanced the heat sinks thermal performance However, the use of materials with changing composition, microstructure, or porosity across the material volume has been proven to be an effective way of improving the thermal performance of heat sink. Such materials with varying electrical, chemical, mechanical, magnetic, and thermal properties over the volume of the bulk material are referred to as functionally graded materials (FGMs). The continuous variations in properties in the FGM along a specific axis could be based on the porosity and pore size gradient structure, chemical gradient structure, and microstructural gradient structure of the FGM.

FGM was initially developed and used for high-temperature applications in Japan during a space plane project [19]. However, their effective thermal, physical, chemical, and magnetic properties have paved ways for their wide range of applications such as engine components, heat shielding of satellites, thermal stress control of cylindrical and spherical bodies, and vessels and several applications in aerospace, automobile, and nuclear industries. Although there are numerous studies in literature on cooling of electronics components using heat sink [20–27], an in-depth examination and review of the past works indicate to the best of our knowledge that FGM has not been applied in heat sinks except in [20]. Recent works on the applications of the non-Fourier heat transfer in extended surfaces, transient analysis of fins under dehumidification, and other optimization studies as well as the recent advancements in Legendre polynomials have been well presented [28–47]. Thus, considering the significant capabilities and benefits of FGM coupled with established enhanced heat transfer characteristics of porous fins. However, different studies on the thermal performance of fins with and without functionally graded materials have been carried out. However, to the best of the authors' knowledge, a study on the transient thermal analysis of fin with functionally graded materials is scarce. Therefore, in this work, nonlinear transient thermal analysis of a convective-radiative fin with functionally graded materials under the influence of magnetic field is presented. The developed nonlinear thermal models of linear, quadratic, and exponential variation of thermal conductivity are solved approximately and analytically using the differential transformation method. This method converges very fast and is very efficient for the handling of both ordinary and partial differential equations. However, when the domain of convergence is at infinity, there is always a need to augment the classical differential transform method with PADE approximants, cosine and sine after treatments, domain transformation, or multistep DTM. In order to verify the accuracies of the nonlinear solutions, exact analytical solutions are also developed with the aids of Bessel, Legendre, and modified Bessel functions. The effects of heat enhancement capacity of fin with the functionally graded material as compared to fin with the homogeneous material are investigated. Also, influence of the Lorentz force and radiative heat transfer on the thermal performance of the fin are analyzed.

2. Problem Formulation

Consider a heat sink made of FGM having length b and thickness t exposed on both faces to a convective-radiative environment at temperature T_∞ as shown in Figure 1, assuming the fin medium is homogeneous, isotropic, and saturated with a single-phase fluid. Moreover, the physical properties of solid as well as fluid are considered as constant, and the temperature variation inside the fin is one-dimensional, i.e., temperature varies along the length only and remain constant with time and there is no thermal contact resistance at the fin base and the fin tip is an adiabatic type.

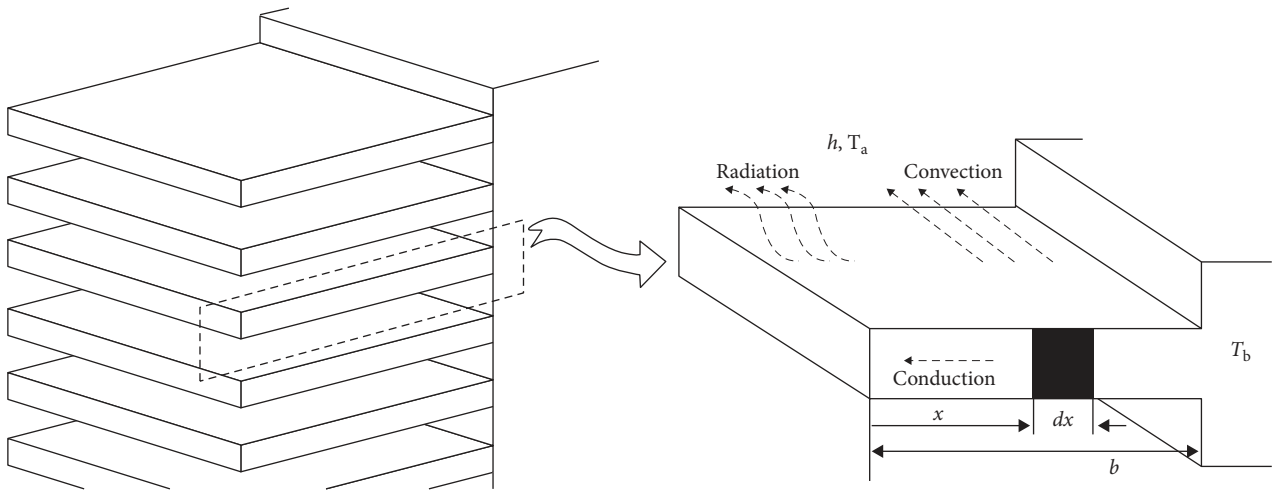

Figure 1: Schematic diagram of heat transfer in a longitudinal fin with FGM.

Following the assumptions, the governing differential equation is developed as

$$\rho c_{\mathrm{p}} \frac{\partial T}{\partial t} = \frac{\partial}{\partial x}\left(k(x)\frac{\partial T}{\partial x}\right) - \frac{hP}{A}\left(T - T_{\mathrm{a}}\right) - \frac{\sigma \varepsilon P}{A}\left(T^4 - T_{\mathrm{a}}^4\right) - \frac{J_{\mathrm{c}} \times J_{\mathrm{c}}}{\sigma A}. \tag{1}$$

But the Lorentz force can be written as

$$\frac{J_{\mathrm{c}} \times J_{\mathrm{c}}}{\sigma} = \sigma B_0^2 u^2. \tag{2}$$

After substitution of equation (2) into equation (1), taking the magnetic term as a linear function of temperature, we have

$$\rho c_{\mathrm{p}} \frac{\partial T}{\partial t} = \frac{\partial}{\partial x}\left(k(x)\frac{\partial T}{\partial x}\right) - \frac{hP}{A}\left(T - T_{\mathrm{a}}\right) - \frac{\sigma \varepsilon P}{A}\left(T^4 - T_{\mathrm{a}}^4\right) - \frac{\sigma B_0^2 u^2}{A}\left(T - T_{\mathrm{a}}\right). \tag{3}$$

Initial condition is stated as

$$t = 0,\ T = T_{\mathrm{a}},\ x > 0, \tag{4}$$

while the boundary conditions are

$$t > 0,\ x = 0,\ \frac{\partial T}{\partial x} = 0,\ t > 0,\ x = L,\ T = T_{\mathrm{b}}. \tag{5}$$

In most practical situations, the fin thickness at the end is small that the heat transfer from the fin tip can be neglected and solution can be obtained assuming fin is insulated at the tip. Therefore, in this work, we assumed that the tip of the fin is adiabatic/insulated.

In the present analysis, cases of linear, quadratic, and exponential variation of thermal conductivity with the fin length will be considered.

Linear variation of thermal conductivity with the fin length:

$$k(x) = k_0\left(1 + \gamma_1 x\right). \tag{6}$$

Quadratic variation of thermal conductivity with the fin length:

$$k(x) = k_0\left(1 + \gamma_q x^2\right). \tag{7}$$

Exponential variation of thermal conductivity with the fin length:

$$k(x) = k_0 e^{\gamma_i x}. \tag{8}$$

It should be noted that when rapid cooling is required in the domain of the FGM fin (such as in the condenser, electronic devices, and CPU), FGM materials with quadratic thermal conductivity variation may be applied. However, if slow heat enhancement is required as in the fluidized bed, exponential is advised. For an intermediate and moderate heat transfer or enhancement process, linear thermal conductivity variation will be useful.

Case 1. Linear variation of thermal conductivity with the fin length:

$$\frac{\rho c_{\mathrm{p}}}{k_0}\frac{\partial T}{\partial t} = \frac{\partial^2 T}{\partial x^2} + \gamma_l x \frac{\partial^2 T}{\partial x^2} + \gamma_l \frac{\partial T}{\partial x} - \frac{hP}{k_0 A}\left(T - T_{\mathrm{a}}\right) - \frac{\sigma \varepsilon P}{A}\left(T^4 - T_{\mathrm{a}}^4\right) - \frac{\sigma B_0^2 u^2}{k_0 A}\left(T - T_{\mathrm{a}}\right). \tag{9}$$

Case 2. Quadratic variation of thermal conductivity with the fin length:

$$\frac{\rho c_{\mathrm{p}}}{k_0}\frac{\partial T}{\partial t} = \frac{\partial^2 T}{\partial x^2} + \gamma_q x^2 \frac{\partial^2 T}{\partial x^2} + 2\gamma_q x \frac{\partial T}{\partial x} - \frac{hP}{k_0 A}\left(T - T_{\mathrm{a}}\right) - \frac{\sigma \varepsilon P}{A}\left(T^4 - T_{\mathrm{a}}^4\right) - \frac{\sigma B_0^2 u^2}{k_0 A}\left(T - T_{\mathrm{a}}\right). \tag{10}$$

Case 3. Exponential variation of thermal conductivity with the fin length:

$$\frac{\rho c_p}{k_0}\frac{\partial T}{\partial t} = e^{\gamma_i x}\frac{\partial^2 T}{\partial x^2} + \gamma_i e^{\gamma_i x}\frac{\partial T}{\partial x} - \frac{hP}{k_0 A}(T - T_a) - \frac{\sigma\varepsilon P}{A}\left(T^4 - T_a^4\right) - \frac{\sigma B_0^2 u^2}{k_0 A}(T - T_a). \tag{11}$$

In order to nondimensionalize the developed governing equations, the following dimensionless parameters are used in equations (9)–(11):

$$X = \frac{x}{L},$$

$$\theta = \frac{T - T_a}{T_b - T_a},$$

$$\tau = \frac{k_0 t}{\rho c_p L^2},$$

$$\beta = \gamma_l L = \gamma_i L,$$

$$\lambda = \beta_q L^2,$$

$$\mathrm{Nc}^2 = \frac{PLh}{Ak_0},$$

$$\mathrm{Nr} = \frac{4\sigma\varepsilon P T_a^3}{k_0 A},$$

$$\mathrm{Ma}^2 = \frac{\sigma B_0^2 u^2}{k_0 A},$$

$$C_T = \frac{T_\infty}{T_b - T_\infty}. \tag{12}$$

Then, the dimensionless forms of the governing equations (9)–(11) can be written as follows.

Case 1. Linear variation of thermal conductivity with the fin length:

$$\frac{\partial\theta}{\partial\tau} = \frac{\partial^2\theta}{\partial X^2} + \beta X\frac{\partial^2\theta}{\partial X^2} + \beta\frac{\partial\theta}{\partial X} - \mathrm{Nc}^2\theta - \mathrm{Nr}\left[(\theta + C_T)^4 - C_T^4\right] - \mathrm{Ma}^2\theta = 0. \tag{13}$$

Case 2. Quadratic variation of thermal conductivity with the fin length:

$$\frac{\partial\theta}{\partial\tau} = \frac{\partial^2\theta}{\partial X^2} + \lambda X^2\frac{\partial^2\theta}{\partial X^2} + 2\lambda X\frac{\partial\theta}{\partial X} - \mathrm{Nc}^2\theta - \mathrm{Nr}\left[(\theta + C_T)^4 - C_T^4\right] - \mathrm{Ma}^2\theta = 0. \tag{14}$$

Case 3. Exponential variation of thermal conductivity with the fin length:

$$\frac{\partial\theta}{\partial\tau} = e^{\beta X}\frac{\partial^2\theta}{\partial X^2} + \beta e^{\beta X}\frac{\partial\theta}{\partial X} - \mathrm{Nc}^2\theta - \mathrm{Nr}\left[(\theta + C_T)^4 - C_T^4\right] - \mathrm{Ma}^2\theta = 0, \tag{15}$$

and the dimensionless initial and boundary conditions are

$$\tau = 0,\ \theta = 0,\ X > 0,\ \tau > 0,\ X = 0,\ \frac{\partial\theta}{\partial X} = 0, \tag{16}$$

$$\tau > 0,\ X = 1,\ \theta = 1. \tag{17}$$

Case 1. Linear variation of thermal conductivity with the fin length:

$$\frac{\partial\theta}{\partial\tau} = \frac{\partial^2\theta}{\partial X^2} + \beta X\frac{\partial^2\theta}{\partial X^2} + \beta\frac{\partial\theta}{\partial X} - \mathrm{Nc}^2\theta - \mathrm{Nr}\theta^4 - 4\mathrm{Nr}C_T\theta^3 - 6\mathrm{Nr}C_T^2\theta^2 - 4\mathrm{Nr}C_T^3\theta - \mathrm{Ma}\theta = 0. \tag{18}$$

Case 2. Quadratic variation of thermal conductivity with the fin length:

$$\frac{\partial\theta}{\partial\tau} = \frac{\partial^2\theta}{\partial X^2} + \lambda X^2\frac{\partial^2\theta}{\partial X^2} + 2\lambda X\frac{\partial\theta}{\partial X} - \mathrm{Nc}^2\theta - \mathrm{Nr}\theta^4 - 4\mathrm{Nr}C_T\theta^3 - 6\mathrm{Nr}C_T^2\theta^2 - 4\mathrm{Nr}C_T^3\theta - \mathrm{Ma}\theta = 0. \tag{19}$$

Case 3. Exponential variation of thermal conductivity with the fin length:

$$\frac{\partial\theta}{\partial\tau} = e^{\beta X}\frac{\partial^2\theta}{\partial X^2} + \beta e^{\beta X}\frac{\partial\theta}{\partial X} - \mathrm{Nc}^2\theta - \mathrm{Nr}\theta^4 - 4\mathrm{Nr}C_T\theta^3 - 6\mathrm{Nr}C_T^2\theta^2 - 4\mathrm{Nr}C_T^3\theta - \mathrm{Ma}\theta = 0. \tag{20}$$

3. Method of Solution for the Nonlinear Thermal Models: Differential Transform Method

The developed nonlinear thermal models in equations (18)–(20) are very difficult to solve exactly and analytically. Therefore, a recourse was made to an approximation analytical method, differential transform method. The basic definitions and the operational properties of the method can be found in our previous study [48].

Case 1. Linear variation of thermal conductivity with the fin length.

The recursive relation for the linear variation of thermal conductivity with the fin length given in equation (20) is

$$
\begin{aligned}
(h+1)\theta[k,h+1] &= (k+1)(k+2)\theta[k+2,h] + \beta\sum_{r=0}^{k}\sum_{u=0}^{h}\delta[r-1,h-u](k-r+1)(k-r+2)\theta[k-r+2,u] \\
&\quad + \beta(k+1)\theta[k+1,h] - \left(\mathrm{Nc}^2+\mathrm{Ma}^2\right)\theta[k,h] \\
&\quad - \mathrm{Nr}\left\{\begin{array}{l}
\displaystyle\sum_{r=0}^{k}\sum_{s=0}^{k-r}\sum_{t=0}^{k-r-s}\sum_{u=0}^{h}\sum_{v=0}^{h-u}\sum_{w=0}^{h-u-v}\theta[r,h-u-v-w]\theta[s,u]\theta[t,v]\theta[k-r-s-t,w]+ \\
\displaystyle 4C_{\mathrm{T}}\sum_{r=0}^{k}\sum_{s=0}^{k-r}\sum_{u=0}^{h}\sum_{v=0}^{h-u}\theta[r,h-u-v]\theta[s,u]\theta[k-r-s,w]+ \\
\displaystyle 6C_{\mathrm{T}}^2\sum_{r=0}^{k}\sum_{u=0}^{h}\theta[r,h-u]\theta[k-r,w]+ \\
4C_{\mathrm{T}}^3\theta[k,h]
\end{array}\right\}.
\end{aligned}
\tag{21}
$$

Using the recursive relation in equation (21), one arrives at

$$
\begin{aligned}
\theta[2,1] &= \sigma + \frac{\mathrm{Ma}^2\sigma}{2} + \frac{\mathrm{Nc}^2\sigma}{2} + 2\mathrm{Nr}\sigma C_{\mathrm{T}}^3, \\
\theta[3,1] &= -\frac{1}{6}\beta\sigma\left(2+\mathrm{Ma}^2+\mathrm{Nc}^2+4\mathrm{Nr}C_{\mathrm{T}}^3\right), \\
\theta[4,1] &= \left\{\frac{\sigma}{4}+\frac{\mathrm{Ma}^2\sigma}{6}+\frac{\mathrm{Ma}^4\sigma}{24}+\frac{\mathrm{Nc}^2\sigma}{6}+\frac{1}{12}\mathrm{Ma}^2\mathrm{Nc}^2\sigma+\frac{\mathrm{Nc}^4\sigma}{24}+\frac{\beta^2\sigma}{12}+\frac{1}{24}\mathrm{Ma}^2\beta^2\sigma+\frac{1}{24}\mathrm{Nc}^2\beta^2\sigma+\frac{1}{2}\mathrm{Nr}\sigma^2C_{\mathrm{T}}^2+\frac{2}{3}\mathrm{Nr}\sigma C_{\mathrm{T}}^3\right. \\
&\quad \left.+\frac{1}{3}\mathrm{Ma}^2\mathrm{Nr}\sigma C_{\mathrm{T}}^3+\frac{1}{3}\mathrm{Nc}^2\mathrm{Nr}\sigma C_{\mathrm{T}}^3+\frac{1}{6}\mathrm{Nr}\beta^2\sigma C_{\mathrm{T}}^3+\frac{2}{3}\mathrm{Nr}^2\sigma C_{\mathrm{T}}^6\right\}, \\
\theta[2,2] &= 2\mathrm{Nr}C_{\mathrm{T}}^3\sigma + 3C_{\mathrm{T}}^2\mathrm{Nr}\sigma^2 + \frac{1}{2}\mathrm{Ma}^2\sigma + \frac{1}{2}\mathrm{Nc}^2\sigma + \frac{3}{2}, \\
\theta[3,2] &= -\frac{1}{6}\beta\sigma\left(3+\mathrm{Nc}^2+\mathrm{Ma}^2+6\mathrm{Nr}\sigma C_{\mathrm{T}}^2+4\mathrm{Nr}C_{\mathrm{T}}^3\right), \\
\theta[5,1] &= \left\{-\frac{\beta\sigma}{10}-\frac{1}{15}\mathrm{Nc}^2\beta\sigma-\frac{1}{60}\mathrm{Nc}^4\beta\sigma-\frac{\beta^3\sigma}{60}-\frac{1}{120}\mathrm{Nc}^2\beta^3\sigma-\frac{1}{15}\beta\sigma\mathrm{Ma}^2-\frac{1}{30}\mathrm{Nc}^2\beta\sigma\mathrm{Ma}^2-\frac{1}{120}\beta^3\sigma\mathrm{Ma}^2-\frac{1}{60}\beta\sigma\mathrm{Ma}^4\right. \\
&\quad \left.-\frac{1}{5}\mathrm{Nr}\beta\sigma^2C_{\mathrm{T}}^2-\frac{4}{15}\mathrm{Nr}\beta\sigma C_{\mathrm{T}}^3-\frac{2}{15}\mathrm{Nc}^2\mathrm{Nr}\beta\sigma C_{\mathrm{T}}^3-\frac{1}{30}\mathrm{Nr}\beta^3\sigma C_{\mathrm{T}}^3-\frac{2}{15}\mathrm{Nr}\beta\sigma\mathrm{Ma}^2C_{\mathrm{T}}^3-\frac{4}{15}\mathrm{Nr}^2\beta\sigma C_{\mathrm{T}}^6\right\}.
\end{aligned}
\tag{22}
$$

Case 2. Quadratic variation of thermal conductivity with the fin length.

The recursive relation for the quadratic variation of thermal conductivity with the fin length given in equation (19) is

$$
\begin{aligned}
(h+1)\theta[k,h+1] &= (k+1)(k+2)\theta[k+2,h] + \lambda\sum_{r=0}^{k}\sum_{u=0}^{h}\delta[r-2,h-u](k-r+1)(k-r+2)\theta[k-r+2,u] \\
&\quad + 2\lambda\sum_{r=0}^{k}\sum_{u=0}^{h}\delta[r-1,h-u](k-r+1)\theta[k-r+1,u] - \left(\mathrm{Nc}^2+\mathrm{Ma}^2\right)\theta[k,h] \\
&\quad - \mathrm{Nr}\left\{\begin{array}{l}
\displaystyle\sum_{r=0}^{k}\sum_{s=0}^{k-r}\sum_{t=0}^{k-r-s}\sum_{u=0}^{h}\sum_{v=0}^{h-u}\sum_{w=0}^{h-u-v}\theta[r,h-u-v-w]\theta[s,u]\theta[t,v]\theta[k-r-s-t,w]+ \\
\displaystyle 4C_{\mathrm{T}}\sum_{r=0}^{k}\sum_{s=0}^{k-r}\sum_{u=0}^{h}\sum_{v=0}^{h-u}\theta[r,h-u-v]\theta[s,u]\theta[k-r-s,w]+ \\
\displaystyle 6C_{\mathrm{T}}^2\sum_{r=0}^{k}\sum_{u=0}^{h}\theta[r,h-u]\theta[k-r,w]+ \\
4C_{\mathrm{T}}^3\theta[k,h]
\end{array}\right\}.
\end{aligned}
\tag{23}
$$

With the aid of the recursive relation in equation (23), we have

$$\begin{aligned}
&\theta[2,1] = \sigma + \frac{\mathrm{Ma}^2\sigma}{2} + \frac{\mathrm{Nc}^2\sigma}{2} + 2\mathrm{Nr}\sigma C_{\mathrm{T}}^3,\\
&\theta[3,1] = 0,\\
&\theta[2,2] = \frac{3\sigma}{2} + \frac{\mathrm{Ma}^2\sigma}{2} + \frac{\mathrm{Nc}^2\sigma}{2} + 3\mathrm{Nr}\sigma^2 C_{\mathrm{T}}^2 + 2\mathrm{Nr}\sigma C_{\mathrm{T}}^3,\\
&\theta[3,2] = 0,\\
&\theta[4,1] = \left\{\frac{\sigma}{4} + \frac{\mathrm{Ma}^2\sigma}{6} + \frac{\mathrm{Ma}^4\sigma}{24} + \frac{\mathrm{Nc}^2\sigma}{6} + \frac{1}{12}\mathrm{Ma}^2\mathrm{Nc}^2\sigma + \frac{\mathrm{Nc}^4\sigma}{24} + \frac{1}{2}\mathrm{Nr}\sigma^2 C_{\mathrm{T}}^2 + \frac{2}{3}\mathrm{Nr}\sigma C_{\mathrm{T}}^3 + \frac{1}{3}\mathrm{Ma}^2\mathrm{Nr}\sigma C_{\mathrm{T}}^3 + \frac{1}{3}\mathrm{Nc}^2\mathrm{Nr}\sigma C_{\mathrm{T}}^3 + \frac{2}{3}\mathrm{Nr}^2\sigma C_{\mathrm{T}}^6\right\},\\
&\theta[5,1] = 0.
\end{aligned} \tag{24}$$

Case 3. Exponential variation of thermal conductivity with the fin length.

The recursive relation for the exponential variation of thermal conductivity with the fin length given in equation (20) is

$$\begin{aligned}
(h+1)\theta[k,h+1] = {} & \sum_{r=0}^{k}\sum_{u=0}^{h}\frac{\beta^r}{r!}\delta[h-u](k-r+1)(k-r+2)\theta[k-r+2,u] + \beta\sum_{r=0}^{k}\sum_{u=0}^{h}\frac{\beta^r}{r!}\delta[h-u](k-r+1)\theta[k-r+1,u]\\
& -\left(\mathrm{Nc}^2+\mathrm{Ma}^2\right)\theta[k,h] - \mathrm{Nr}\left\{\begin{array}{l}
\displaystyle\sum_{r=0}^{k}\sum_{s=0}^{k-r}\sum_{t=0}^{k-r-s}\sum_{u=0}^{h}\sum_{v=0}^{h-u}\sum_{w=0}^{h-u-v}\theta[r,h-u-v-w]\theta[s,u]\theta[t,v]\theta[k-r-s-t,w]+\\
\displaystyle 4C_{\mathrm{T}}\sum_{r=0}^{k}\sum_{s=0}^{k-r}\sum_{u=0}^{h}\sum_{v=0}^{h-u}\theta[r,h-u-v]\theta[s,u]\theta[k-r-s,w]+\\
\displaystyle 6C_{\mathrm{T}}^2\sum_{r=0}^{k}\sum_{u=0}^{h}\theta[r,h-u]\theta[k-r,w]+\\
4C_{\mathrm{T}}^3\theta[k,h]
\end{array}\right\}.
\end{aligned} \tag{25}$$

From the recursive relation in equation (25), one arrives at

$$\begin{aligned}
&\theta[2,1] = \sigma + \frac{\mathrm{Ma}^2\sigma}{2} + \frac{\mathrm{Nc}^2\sigma}{2} + 2\mathrm{Nr}\sigma C_{\mathrm{T}}^3,\\
&\theta[3,1] = -\frac{2\beta\sigma}{3} - \frac{1}{3}\mathrm{Ma}^2\beta\sigma - \frac{1}{3}\mathrm{Nc}^2\beta\sigma - \frac{4}{3}\mathrm{Nr}\beta\sigma C_{\mathrm{T}}^3,\\
&\theta[2,2] = \frac{3\sigma}{2} + \frac{\mathrm{Ma}^2\sigma}{2} + \frac{\mathrm{Nc}^2\sigma}{2} + 3\mathrm{Nr}\sigma^2 C_{\mathrm{T}}^2 + 2\mathrm{Nr}\sigma C_{\mathrm{T}}^3,\\
&\theta[3,2] = -\beta\sigma - \frac{1}{3}\mathrm{Ma}^2\beta\sigma - \frac{1}{3}\mathrm{Nc}^2\beta\sigma - 2\mathrm{Nr}\beta\sigma^2 C_{\mathrm{T}}^2 - \frac{4}{3}\mathrm{Nr}\beta\sigma C_{\mathrm{T}}^3,\\
&\theta[4,1] = \left\{\frac{\sigma}{4} + \frac{\mathrm{Ma}^2\sigma}{6} + \frac{\mathrm{Ma}^4\sigma}{24} + \frac{\mathrm{Nc}^2\sigma}{6} + \frac{1}{12}\mathrm{Ma}^2\mathrm{Nc}^2\sigma + \frac{\mathrm{Nc}^4\sigma}{24} + \frac{\beta^2\sigma}{4} + \frac{1}{8}\mathrm{Ma}^2\beta^2\sigma + \frac{1}{8}\mathrm{Nc}^2\beta^2\sigma + \frac{1}{2}\mathrm{Nr}\sigma^2 C_{\mathrm{T}}^2 + \frac{2}{3}\mathrm{Nr}\sigma C_{\mathrm{T}}^3\right.\\
&\qquad \left. + \frac{1}{3}\mathrm{Ma}^2\mathrm{Nr}\sigma C_{\mathrm{T}}^3 + \frac{1}{3}\mathrm{Nc}^2\mathrm{Nr}\sigma C_{\mathrm{T}}^3 + \frac{1}{2}\mathrm{Nr}\beta^2\sigma C_{\mathrm{T}}^3 + \frac{2}{3}\mathrm{Nr}^2\sigma C_{\mathrm{T}}^6\right\},\\
&\theta[5,1] = \left\{-\frac{3\beta\sigma}{10} - \frac{1}{5}\mathrm{Ma}^2\beta\sigma - \frac{1}{20}\mathrm{Ma}^4\beta\sigma - \frac{1}{5}\mathrm{Nc}^2\beta\sigma - \frac{1}{10}\mathrm{Ma}^2\mathrm{Nc}^2\beta\sigma - \frac{1}{20}\mathrm{Nc}^4\beta\sigma - \frac{\beta^3\sigma}{15} - \frac{1}{30}\mathrm{Ma}^2\beta^3\sigma - \frac{1}{30}\mathrm{Nc}^2\beta^3\sigma - \frac{3}{5}\mathrm{Nr}\beta\sigma^2 C_{\mathrm{T}}^2\right.\\
&\qquad \left. - \frac{4}{5}\mathrm{Nr}\beta\sigma C_{\mathrm{T}}^3 - \frac{2}{5}\mathrm{Ma}^2\mathrm{Nr}\beta\sigma C_{\mathrm{T}}^3 - \frac{2}{5}\mathrm{Nc}^2\mathrm{Nr}\beta\sigma C_{\mathrm{T}}^3 - \frac{2}{15}\mathrm{Nr}\beta^3\sigma C_{\mathrm{T}}^3 - \frac{4}{5}\mathrm{Nr}^2\beta\sigma C_{\mathrm{T}}^6\right\}.
\end{aligned} \tag{26}$$

4. Development of Exact Analytical Solution for the Linearized Thermal Models

In order to verify the accuracies of the nonlinear solutions as developed in the previous sections, exact analytical solutions are also developed. In order to do this, we considered a case where the temperature difference within the material during the heat flow is small. Under such scenario, the adoption of temperature-invariant physical and thermal properties of the fin and expression T^4 as a linear function of temperature can be done without any loss of generality and accuracy:

$$T^4 \cong 4T_a^3 T - 3T_a^4. \tag{27}$$

On substituting equation (27) into equation (9), we arrived at the following equation:

$$\rho c_p \frac{\partial T}{\partial t} = \frac{\partial}{\partial x}\left(k(x)\frac{\partial T}{\partial x}\right) - \frac{hP}{A}(T - T_a) - \frac{4\sigma\varepsilon P T_a^3}{A}(T - T_a) - \frac{\sigma B_0^2 u^2}{A}(T - T_a). \tag{28}$$

Upon substitution of equations (6)–(8) into equation (28) and expanding the resulting equations, we have the following.

Case 1. Linear variation of thermal conductivity with the fin length:

$$\frac{\rho c_p}{k_0}\frac{\partial T}{\partial t} = \frac{\partial^2 T}{\partial x^2} + \gamma_l x\frac{\partial^2 T}{\partial x^2} + \gamma_l \frac{\partial T}{\partial x} - \frac{hP}{k_0 A}(T - T_a) - \frac{4\sigma\varepsilon P T_a^3}{k_0 A}(T - T_a) - \frac{\sigma B_0^2 u^2}{k_0 A}(T - T_a). \tag{29}$$

Case 2. Quadratic variation of thermal conductivity with the fin length:

$$\frac{\rho c_p}{k_0}\frac{\partial T}{\partial t} = \frac{\partial^2 T}{\partial x^2} + \gamma_q x^2\frac{\partial^2 T}{\partial x^2} + 2\gamma_q x\frac{\partial T}{\partial x} - \frac{hP}{k_0 A}(T - T_a) - \frac{4\sigma\varepsilon P T_a^3}{k_0 A}(T - T_a) - \frac{\sigma B_0^2 u^2}{k_0 A}(T - T_a). \tag{30}$$

Case 3. Exponential variation of thermal conductivity with the fin length:

$$\frac{\rho c_p}{k_0}\frac{\partial T}{\partial t} = e^{\gamma_i x}\frac{\partial^2 T}{\partial x^2} + \gamma_i e^{\gamma_i x}\frac{\partial T}{\partial x} - \frac{hP}{k_0 A}(T - T_a) - \frac{4\sigma\varepsilon P T_a^3}{k_0 A}(T - T_a) - \frac{\sigma B_0^2 u^2}{k_0 A}(T - T_a). \tag{31}$$

Applying the nondimensionalize parameters in equation (12) to equations (29)–(31), we obtain the dimensionless forms of the linearized governing equations as given below.

Case 1. Linear variation of thermal conductivity with the fin length:

$$\frac{\partial \theta}{\partial \tau} = \frac{\partial^2 \theta}{\partial X^2} + \beta X\frac{\partial^2 \theta}{\partial X^2} + \beta\frac{\partial \theta}{\partial X} - \mathrm{Nc}^2\theta - \mathrm{Nr}\theta - \mathrm{Ma}^2\theta. \tag{32}$$

Case 2. Quadratic variation of thermal conductivity with the fin length:

$$\frac{\partial \theta}{\partial \tau} = \frac{\partial^2 \theta}{\partial X^2} + \lambda X^2\frac{\partial^2 \theta}{\partial X^2} + 2\lambda X\frac{\partial \theta}{\partial X} - \mathrm{Nc}^2\theta - \mathrm{Nr}\theta - \mathrm{Ma}^2\theta. \tag{33}$$

Case 3. Exponential variation of thermal conductivity with the fin length:

$$\frac{\partial \theta}{\partial \tau} = e^{\beta X}\frac{\partial^2 \theta}{\partial X^2} + \beta e^{\beta X}\frac{\partial \theta}{\partial X} - \mathrm{Nc}^2\theta - \mathrm{Nr}\theta - \mathrm{Ma}^2\theta, \tag{34}$$

and the dimensionless initial and boundary conditions are

$$\tau = 0,\ \theta = 0,\ X > 0,\ \tau > 0,\ X = 0,\ \frac{\partial \theta}{\partial X} = 0,\ \tau > 0,\ X = 1,\ \theta = 1. \tag{35}$$

4.1. Method of Solution Using Laplace Transform Method. In order to provide closed-form solutions to the developed equations, we adopted integral transforms using Laplace transform. We first apply Laplace transform over the time and then solve the resulting equation using Bessel, modified Bessel, Legendre, and sign and gamma functions. The procedures are given as follows:

The Laplace transform of a real function $f(t)$ and its inversion formulas are defined as follows:

$$F(s) = \int_0^\infty e^{-st} f(t)dt, \qquad f(t) = \frac{1}{2\pi i}\int_{s-i\infty}^{s+i\infty} e^{-st}F(s)\,dt, \tag{36}$$

where $s = a + ib\,(a, b \in R)$ is a complex number.

Applying Laplace transform on equations (15)–(17), we have the equation in Laplace domain as follows.

Case 1. Linear variation of thermal conductivity with the fin length:

$$\frac{d^2\widetilde{\theta}}{dX^2} + \beta X\frac{d^2\widetilde{\theta}}{dX^2} + \beta\frac{d\widetilde{\theta}}{dX} - \left(s + \mathrm{Nc}^2 + \mathrm{Nr} + \mathrm{Ma}^2\right)\widetilde{\theta}. \tag{37}$$

Case 2. Quadratic variation of thermal conductivity with the fin length:

$$\frac{d^2\widetilde{\theta}}{dX^2} + \lambda X^2\frac{d^2\widetilde{\theta}}{dX^2} + 2\lambda X\frac{d\widetilde{\theta}}{dX} - \left(s + \mathrm{Nc}^2 + \mathrm{Nr} + \mathrm{Ma}^2\right)\widetilde{\theta}. \tag{38}$$

Case 3. Exponential variation of thermal conductivity with the fin length:

$$e^{\beta X}\frac{d^2\widetilde{\theta}}{dX^2} + \beta e^{\beta X}\frac{d\widetilde{\theta}}{dX} - \left(s + \mathrm{Nc}^2 + \mathrm{Nr} + \mathrm{Ma}^2\right)\widetilde{\theta}, \tag{39}$$

and the dimensionless initial and boundary conditions in Laplace domain are

$$s = 0,\ \widetilde{\theta} = 0,\ X > 0, \tag{40}$$

$$s > 0,\ X = 0,\ \frac{\partial \widetilde{\theta}}{\partial X} = 0,\ s > 0,\ X = 1,\ \theta = \frac{1}{s}. \tag{41}$$

With the aids of Bessel, modified Bessel, Legendre, and sign and gamma functions, it could be shown that the solutions of equations (37)–(39) are as follows.

Case 1. Linear variation of thermal conductivity with the fin length:

$$\widetilde{\theta}(X,s) = \left\{J_0\left((2/\beta)\sqrt{-(s+\mathrm{Nc}^2+\mathrm{Nr}+\mathrm{Ma}^2)(1+\beta X)}\right)Y_1\left(2c\mathrm{sgn}(1/\beta)(1/\beta)\sqrt{-(s+\mathrm{Nc}^2+\mathrm{Nr}+\mathrm{Ma}^2)}\right)\right.$$
$$- Y_0\left((2/\beta)\sqrt{-(s+\mathrm{Nc}^2+\mathrm{Nr}+\mathrm{Ma}^2)(1+\beta X)}\right)J_1\left(2c\mathrm{sgn}(1/\beta)(1/\beta)\sqrt{-(s+\mathrm{Nc}^2+\mathrm{Nr}+\mathrm{Ma}^2)}\right)\Big\} \times \Big\{J_0\left((2/\beta)\sqrt{-(s+\mathrm{Nc}^2+\mathrm{Nr}+\mathrm{Ma}^2)}\right)$$
$$\cdot Y_1\left(2c\mathrm{sgn}(1/\beta)(1/\beta)\sqrt{-(s+\mathrm{Nc}^2+\mathrm{Nr}+\mathrm{Ma}^2)}\right) - Y_0\left((2/\beta)\sqrt{-(s+\mathrm{Nc}^2+\mathrm{Nr}+\mathrm{Ma}^2)}\right)J_1\left(2c\mathrm{sgn}(1/\beta)(1/\beta)\sqrt{-(s+\mathrm{Nc}^2+\mathrm{Nr}+\mathrm{Ma}^2)}\right)\Big\}^{-1}. \tag{42}$$

Case 2. Quadratic variation of thermal conductivity with the fin length:

$$\widetilde{\theta}(X,s) = \frac{\left\{\sqrt{\pi}\,Q_n\left(\sqrt{-(\lambda X)}\right) - \Gamma(-(n/2))\Gamma(p/2)Q_m(0)P_n\left(\sqrt{-(\lambda X)}\right)\right\}}{\left\{\sqrt{\pi}\,Q_n\left(\sqrt{-(\lambda)}\right) - \Gamma(-(n/2))\Gamma(p/2)Q_m(0)P_n\left(\sqrt{-(\lambda)}\right)\right\}}, \tag{43}$$

where

$$m = \frac{\sqrt{\lambda + 4\left(s+\mathrm{Nc}^2+\mathrm{Nr}+\mathrm{Ma}^2\right)} + \sqrt{\lambda}}{2\sqrt{\lambda}},$$
$$n = \frac{\sqrt{\lambda + 4\left(s+\mathrm{Nc}^2+\mathrm{Nr}+\mathrm{Ma}^2\right)} - \sqrt{\lambda}}{2\sqrt{\lambda}}, \tag{44}$$
$$p = \frac{\sqrt{\lambda + 4\left(s+\mathrm{Nc}^2+\mathrm{Nr}+\mathrm{Ma}^2\right)} + 5\sqrt{\lambda}}{2\sqrt{\lambda}}.$$

Case 3. Exponential variation of thermal conductivity with the fin length:

$$\widetilde{\theta}(X,s) = e^{-(\beta(X-1)/2)}\left\{K_0\left((2/\beta)\sqrt{(s+\mathrm{Nc}^2+\mathrm{Nr}+\mathrm{Ma}^2)}\right)I_1\left((2/\beta)\sqrt{(s+\mathrm{Nc}^2+\mathrm{Nr}+\mathrm{Ma}^2)}\,e^{-((\beta X)/2)}\right) + I_0\left((2/\beta)\sqrt{(s+\mathrm{Nc}^2+\mathrm{Nr}+\mathrm{Ma}^2)}\right)\right.$$
$$\cdot K_1\left((2/\beta)\sqrt{(s+\mathrm{Nc}^2+\mathrm{Nr}+\mathrm{Ma}^2)}\,e^{-((\beta X)/2)}\right)\Big\} \times \Big\{K_0\left((2/\beta)\sqrt{(s+\mathrm{Nc}^2+\mathrm{Nr}+\mathrm{Ma}^2)}\right)I_1\left((2/\beta)\sqrt{(s+\mathrm{Nc}^2+\mathrm{Nr}+\mathrm{Ma}^2)}\right)e^{-(\beta/2)}$$
$$\left. + I_0\left((2/\beta)\sqrt{(s+\mathrm{Nc}^2+\mathrm{Nr}+\mathrm{Ma}^2)}\right)K_1\left((2/\beta)\sqrt{(s+\mathrm{Nc}^2+\mathrm{Nr}+\mathrm{Ma}^2)}\right)e^{-(\beta/2)}\right\}^{-1}. \tag{45}$$

It should be noted that the first and second kinds of Bessel, modified Bessel, and Legendre functions are given as follows:

$$J_\nu(z) = \sum_{r=0}^{\infty}\frac{(-1)^r(z/2)^{2r+\nu}}{r!\Gamma(\nu+r+1)},$$
$$Y_\nu(z) = \frac{2}{\pi}\left(\sum_{r=0}^{\infty}\frac{(-1)^r(z/2)^{2r+\nu}}{r!\Gamma(\nu+r+1)}\right)\ln\left(\frac{z}{2}\right) - \frac{1}{\pi}\sum_{r=0}^{\infty}\frac{(\nu-r-1)!(z/2)^{2r-\nu}}{r!} - \frac{1}{\pi}\sum_{r=0}^{\infty}\frac{(-1)^r(z/2)^{2r+n}}{r!(r+n)!}[\psi(r+\nu+1)+\psi(r+1)],$$
$$I_\nu(z) = \sum_{r=0}^{\infty}\frac{(z/2)^{2r+\nu}}{r!\Gamma(\nu+r+1)},$$
$$K_\nu(z) = (-1)^{\nu+1}\left(\sum_{r=0}^{\infty}\frac{(z/2)^{2r+\nu}}{r!\Gamma(\nu+r+1)}\right)\ln\left(\frac{z}{2}\right) + \frac{1}{2}\sum_{r=0}^{\infty}\frac{(\nu-r-1)!(z/2)^{2r-\nu}}{r!} + \frac{1}{2}(-1)^\nu\sum_{r=0}^{\infty}\frac{(-1)^r(z/2)^{2r+n}}{r!(r+n)!}[\psi(r+\nu+1)+\psi(r+1)],$$
$$P_\nu(z) = \frac{1}{2^\nu\nu!}\frac{d}{dx^\nu}(x-1)^\nu = 2^\nu\sum_{r=0}^{\nu}x^r\binom{\nu}{r}\binom{\frac{\nu+r-1}{2}}{r}, \tag{46}$$
$$Q_\nu(z) = \frac{1}{2}P_\nu(z)\ln\left(\frac{1+z}{1-z}\right) = 2^{\nu-1}\sum_{r=0}^{\nu}x^r\binom{\nu}{r}\binom{\frac{\nu+r-1}{2}}{r}\ln\left(\frac{1+z}{1-z}\right),$$
$$\psi(r+1) = -\gamma + \sum_{r=1}^{n}\frac{1}{m},$$
$$c\mathrm{sgn}(z) = \begin{bmatrix}1, & \text{if } \mathrm{Re}(z)>0\\ -1, & \text{if } \mathrm{Re}(z)<0\\ \mathrm{sgn}(\mathrm{Im}(z)), & \text{if } \mathrm{Re}(z)=0\end{bmatrix},$$
$$\mathrm{sgn}(z) = \frac{z}{|z|}.$$

It should be noted that ψ is a digamma function while γ is the Euler–Mascheroni constant and c sgn is a sign function for real and complex expressions.

The determination of the inverse Laplace transforms of equations (41)–(43) and (45) is very complex. However, they can be numerically evaluated using Simon's approach [49] given as

$$\theta(X,\tau) = \frac{e^{a_p\tau}}{\tau}\left[\frac{1}{2}\widetilde{\theta}\left(X, a_p\right) + \sum_{n=1}^{N} \mathrm{Re}\left[\widetilde{\theta}\left(X, a_p + i\frac{n\pi}{\tau}\right)\right](-1)^n\right]. \tag{47}$$

Lee et al. [50] suggested values of $a_p\tau$ ranging between 4 and 5. Equations (41)–(43) and (45) converge more quickly because it does not contain oscillating cosine and sine functions.

The optimally value is [50]

$$a_p\tau = 4.7 \Rightarrow a_p = \frac{4.7}{\tau}. \tag{48}$$

Case 1. Linear variation of thermal conductivity with the fin length:

$$\begin{aligned}
\theta(X,\tau) = \frac{e^{a_p\tau}}{\tau}\Bigg[\frac{1}{2}\Bigg\{&J_0\left((2/\beta)\sqrt{-((4.7/\tau)+\mathrm{Nc}^2+\mathrm{Nr}+\mathrm{Ma}^2)(1+\beta X)}\right)Y_1\left(2c\,\mathrm{sgn}(1/\beta)(1/\beta)\sqrt{-((4.7/\tau)+\mathrm{Nc}^2+\mathrm{Nr}+\mathrm{Ma}^2)}\right)\\
&- Y_0\left((2/\beta)\sqrt{-((4.7/\tau)+\mathrm{Nc}^2+\mathrm{Nr}+\mathrm{Ma}^2)(1+\beta X)}\right)J_1\left(2c\,\mathrm{sgn}(1/\beta)(1/\beta)\sqrt{-((4.7/\tau)+\mathrm{Nc}^2+\mathrm{Nr}+\mathrm{Ma}^2)}\right)\Bigg\}\\
&\times\Bigg\{J_0\left((2/\beta)\sqrt{-((4.7/\tau)+\mathrm{Nc}^2+\mathrm{Nr}+\mathrm{Ma}^2)}\right)Y_1\left(2c\,\mathrm{sgn}(1/\beta)(1/\beta)\sqrt{-((4.7/\tau)+\mathrm{Nc}^2+\mathrm{Nr}+\mathrm{Ma}^2)}\right)\\
&- Y_0\left((2/\beta)\sqrt{-((4.7/\tau)+\mathrm{Nc}^2+\mathrm{Nr}+\mathrm{Ma}^2)}\right)J_1\left(2c\,\mathrm{sgn}(1/\beta)(1/\beta)\sqrt{-((4.7/\tau)+\mathrm{Nc}^2+\mathrm{Nr}+\mathrm{Ma}^2)}\right)\Bigg\}^{-1}\\
&+\sum_{n=1}^{N}\mathrm{Re}\Bigg[\Bigg\{J_0\left((2/\beta)\sqrt{-((1/\tau)(4.7+in\pi)+\mathrm{Nc}^2+\mathrm{Nr}+\mathrm{Ma}^2)(1+\beta X)}\right)\\
&\cdot Y_1\left(2c\,\mathrm{sgn}(1/\beta)(1/\beta)\sqrt{-((1/\tau)(4.7+in\pi)+\mathrm{Nc}^2+\mathrm{Nr}+\mathrm{Ma}^2)}\right) - Y_0\left((2/\beta)\sqrt{-((1/\tau)(4.7+in\pi)+\mathrm{Nc}^2+\mathrm{Nr}+\mathrm{Ma}^2)(1+\beta X)}\right)\\
&\cdot J_1\left(2c\,\mathrm{sgn}(1/\beta)(1/\beta)\sqrt{-((1/\tau)(4.7+in\pi)+\mathrm{Nc}^2+\mathrm{Nr}+\mathrm{Ma}^2)}\right)\Bigg\}\times\Bigg\{J_0\left((2/\beta)\sqrt{-((1/\tau)(4.7+in\pi)+\mathrm{Nc}^2+\mathrm{Nr}+\mathrm{Ma}^2)}\right)\\
&\cdot Y_1\left(2c\,\mathrm{sgn}(1/\beta)(1/\beta)\sqrt{-((1/\tau)(4.7+in\pi)+\mathrm{Nc}^2+\mathrm{Nr}+\mathrm{Ma}^2)}\right) - Y_0\left((2/\beta)\sqrt{-((1/\tau)(4.7+in\pi)+\mathrm{Nc}^2+\mathrm{Nr}+\mathrm{Ma}^2)}\right)\\
&\cdot J_1\left(2c\,\mathrm{sgn}(1/\beta)(1/\beta)\sqrt{-((1/\tau)(4.7+in\pi)+\mathrm{Nc}^2+\mathrm{Nr}+\mathrm{Ma}^2)}\right)\Bigg\}^{-1}\Bigg](-1)^n\Bigg].
\end{aligned} \tag{49}$$

Case 2. Quadratic variation of thermal conductivity with the fin length:

$$\theta(X,\tau) = \frac{e^{a_p\tau}}{\tau}\left[\frac{1}{2}\widetilde{\theta}\left(X, a_p\right) + \sum_{n=1}^{N} \mathrm{Re}\left[\widetilde{\theta}\left(X, a_p + i\frac{n\pi}{\tau}\right)\right](-1)^n\right], \tag{50}$$

where

$$\begin{aligned}
\widetilde{\theta}\left(X, a_p\right) &= \frac{\left\{\sqrt{\pi}\,Q_{n'}\left(\sqrt{-(\lambda X)}\right) - \Gamma\left(-(n'/2)\right)\Gamma\left(p'/2\right)Q_{m'}(0)P_{n'}\left(\sqrt{-(\lambda X)}\right)\right\}}{\left\{\sqrt{\pi}\,Q_{n'}\left(\sqrt{-(\lambda)}\right) - \Gamma\left(-(n'/2)\right)\Gamma\left(p'/2\right)Q_{m'}(0)P_{n'}\left(\sqrt{-(\lambda)}\right)\right\}},\\
m' &= \frac{\sqrt{\lambda + 4\left((4.7/\tau)+\mathrm{Nc}^2+\mathrm{Nr}+\mathrm{Ma}^2\right)} + \sqrt{\lambda}}{2\sqrt{\lambda}},\\
n' &= \frac{\sqrt{\lambda + 4\left((4.7/\tau)+\mathrm{Nc}^2+\mathrm{Nr}+\mathrm{Ma}^2\right)} - \sqrt{\lambda}}{2\sqrt{\lambda}},\\
p' &= \frac{\sqrt{\lambda + 4\left((4.7/\tau)+\mathrm{Nc}^2+\mathrm{Nr}+\mathrm{Ma}^2\right)} + 5\sqrt{\lambda}}{2\sqrt{\lambda}}.
\end{aligned} \tag{51}$$

Case 3. Exponential variation of thermal conductivity with the fin length:

$$\theta(X,\tau) = \frac{e^{a_p\tau}}{\tau}\left[\frac{1}{2}e^{-(\beta(X-1)/2)}\left\{K_0\left((2/\beta)\sqrt{((4.7/\tau)+\mathrm{Nc}^2+\mathrm{Nr}+\mathrm{Ma}^2)}\right)I_1\left((2/\beta)\sqrt{((4.7/\tau)+\mathrm{Nc}^2+\mathrm{Nr}+\mathrm{Ma}^2)}\,e^{-((\beta X)/2)}\right)\right.\right.$$
$$\left.+ I_0\left((2/\beta)\sqrt{((4.7/\tau)+\mathrm{Nc}^2+\mathrm{Nr}+\mathrm{Ma}^2)}\right)K_1\left((2/\beta)\sqrt{((4.7/\tau)+\mathrm{Nc}^2+\mathrm{Nr}+\mathrm{Ma}^2)}\,e^{-((\beta X)/2)}\right)\right\}$$
$$\times\left\{K_0\left((2/\beta)\sqrt{((4.7/\tau)+\mathrm{Nc}^2+\mathrm{Nr}+\mathrm{Ma}^2)}\right)I_1\left((2/\beta)\sqrt{((4.7/\tau)+\mathrm{Nc}^2+\mathrm{Nr}+\mathrm{Ma}^2)}\right)e^{-(\beta/2)}\right.$$
$$\left.+ I_0\left((2/\beta)\sqrt{((4.7/\tau)+\mathrm{Nc}^2+\mathrm{Nr}+\mathrm{Ma}^2)}\right)K_1\left((2/\beta)\sqrt{((4.7/\tau)+\mathrm{Nc}^2+\mathrm{Nr}+\mathrm{Ma}^2)}\right)e^{-(\beta/2)}\right\}^{-1}$$
$$+\sum_{n=1}^{N}\mathrm{Re}\left[e^{-(\beta(X-1)/2)}\left\{K_0\left((2/\beta)\sqrt{((1/\tau)(4.7+in\pi)+\mathrm{Nc}^2+\mathrm{Nr}+\mathrm{Ma}^2)}\right)\right.\right.$$
$$\cdot I_1\left((2/\beta)\sqrt{((1/\tau)(4.7+in\pi)+\mathrm{Nc}^2+\mathrm{Nr}+\mathrm{Ma}^2)}\,e^{-((\beta X)/2)}\right)+I_0\left((2/\beta)\sqrt{((1/\tau)(4.7+in\pi)+\mathrm{Nc}^2+\mathrm{Nr}+\mathrm{Ma}^2)}\right)$$
$$\left.\cdot K_1\left((2/\beta)\sqrt{((1/\tau)(4.7+in\pi)+\mathrm{Nc}^2+\mathrm{Nr}+\mathrm{Ma}^2)}\,e^{-((\beta X)/2)}\right)\right\}$$
$$\times\left[\left\{K_0\left((2/\beta)\sqrt{((1/\tau)(4.7+in\pi)+\mathrm{Nc}^2+\mathrm{Nr}+\mathrm{Ma}^2)}\right)I_1\left((2/\beta)\sqrt{((1/\tau)(4.7+in\pi)+\mathrm{Nc}^2+\mathrm{Nr}+\mathrm{Ma}^2)}\right)e^{-(\beta/2)}\right.\right.$$
$$\left.\left.+ I_0\left((2/\beta)\sqrt{((1/\tau)(4.7+in\pi)+\mathrm{Nc}^2+\mathrm{Nr}+\mathrm{Ma}^2)}\right)K_1\left((2/\beta)\sqrt{((1/\tau)(4.7+in\pi)+\mathrm{Nc}^2+\mathrm{Nr}+\mathrm{Ma}^2)}\right)e^{-(\beta/2)}\right\}^{-1}\right](-1)^n\Bigg]. \tag{52}$$

For homogenous material (HM), $\beta = 0$. The solution for the homogeneous material using Laplace transform is given as

$$\theta(X,\tau) = \frac{\cosh\left(\sqrt{\mathrm{Nc}^2+\mathrm{Nr}+\mathrm{Ma}^2}\right)X}{\cosh\left(\sqrt{\mathrm{Nc}^2+\mathrm{Nr}+\mathrm{Ma}^2}\right)} + \frac{4}{\pi}\sum_{n=1}^{\infty}\left(\frac{(-1)^n}{2n-1}\right)e^{-\left(\left(\left((2n-1)^2\pi^2\right)/4\right)+\mathrm{Nc}^2+\mathrm{Nr}+\mathrm{Ma}^2\right)\tau} \cdot \cos\left(\frac{(2n-1)\pi X}{2}\right). \tag{53}$$

5. Results and Discussion

The results of the exact analytical solutions of the fin with the functionally graded material are shown in Figures 2–8. The influences of magnetic field, thermal radiation, inhomogeneity index, and the temperature distribution and history are investigated.

Figures 2–4 show the effects of varying time on the temperature distribution on the FGM fin with variable thermal conductivity according to linear-, quadratic-, and exponential-law functions, respectively. We observe that the temperature increases with an increase in time. The solution seems to converge to a steady state solution as time evolves. We also notice that temperature at the tip of the fin increases with time.

Also, it is depicted in the figure, the time required to cool down to the ambient temperature for all the FGM fins of the variable thermal conductivities considered. The FGM fin with quadratic-law and exponential-law functions shows the slowest and fasted thermal responses, respectively. It is illustrated that, in such cooling down process of the fin, the FGM fin with exponential-law function requires small time to reach steady state than the linear- and quadratic-law functions.

Figures 5(a)–5(d) show the variation of temperature with length at difference dimensionless time for linear-, quadratic-, and exponential-law functions. It is depicted in the figure that the variation of FGM fin thermal conductivity according to the linear law shows an enhanced performance as compared to the quadratic- and exponential-law functions. These enhancements in the energy saving of FGM heat sinks in both linear, quadratic, and exponential laws depict some advantages in the cooling of thermal systems as this causes the lower airflow rate around the heat sinks which results to the smaller fan size and lower electrical energy consumption [16]. The other benefit of smaller fan size is a reduction on the airflow rate within such sensitive devices and controlling the acoustic level, which results to lower distortions, and increasing the electrical or computer component lifetimes.

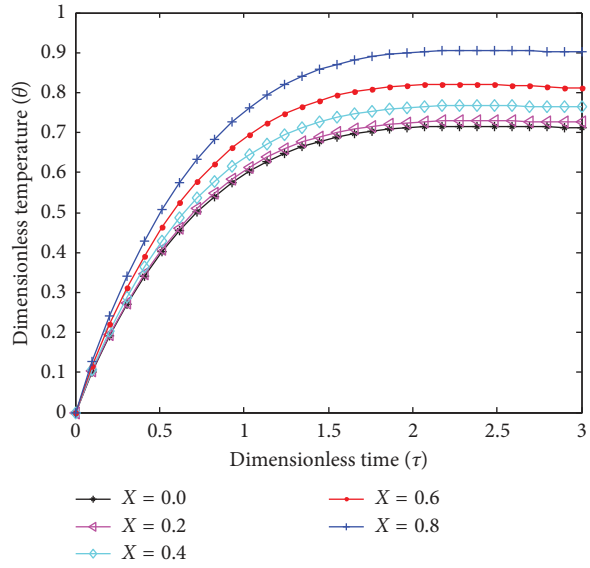

Figure 2: Temperature history in the fin at various locations when the thermal conductivity varies according to linear-law function.

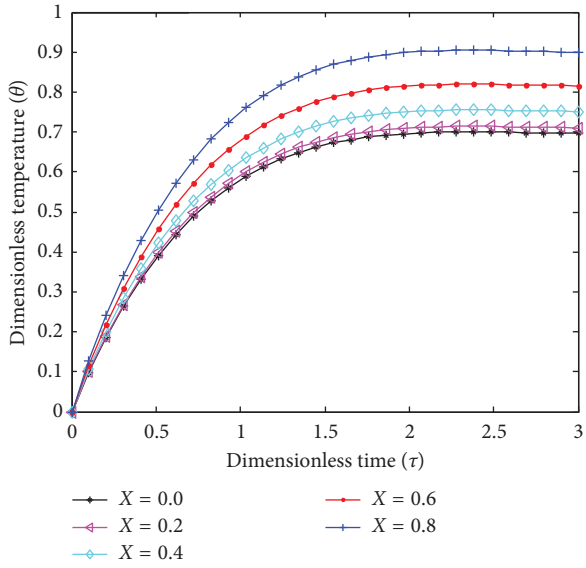

Figure 3: Temperature history in the fin at various locations when the thermal conductivity varies according to quadratic-law function.

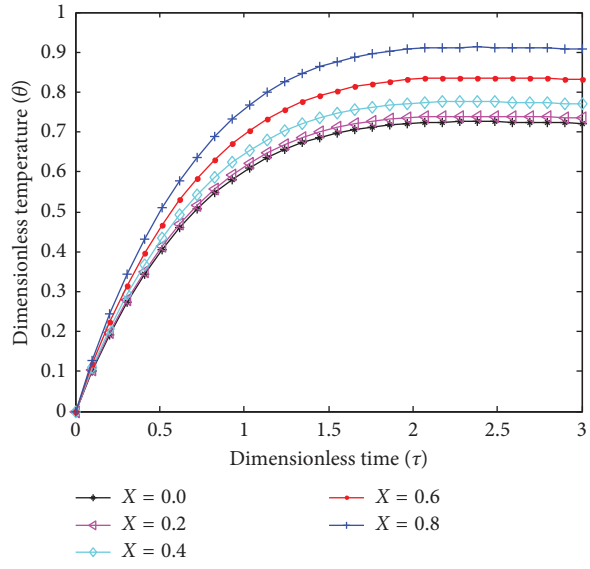

Figure 4: Temperature history in the fin at various locations when the thermal conductivity varies according to exponential-law function.

Figures 6 and 7 illustrate the impacts of magnetic field (Lorentz force) and radiation number on the temperature distribution in the FGM fin. From the figures, as the magnetic field and radiation parameters increase, the temperature decreases rapidly and the rate of heat transfer through the fin increases as the temperature in the fin drops faster as depicted in the figures. The occurrence of rapid decrease in fin temperature as the magnetic parameter is increased is because the augmentation of the Hartmann number causes the force created by the magnetic field to increase which consequently increases the magnetic field strength and created a reduction in the fin temperature. The illustration shows the thermal efficiency of the fin is enhanced by the magnetic force and thermal radiation is induced in the heat transfer process.

As it is displayed, Figures 8(a) and 8(b) show the effects of the in-homogeneity index on the dimensionless temperature distribution and consequently on the rate of heat transfer. From the figures, it is shown that as the in-homogeneity index increases, the rate of heat transfer through the fin increases. For all the values of convective, magnetic field, and radiative parameters, the temperature gradient along the fin with FGM is smaller than the fin with homogeneous material for both linear- and exponential-law functions. Moreover, increasing the in-

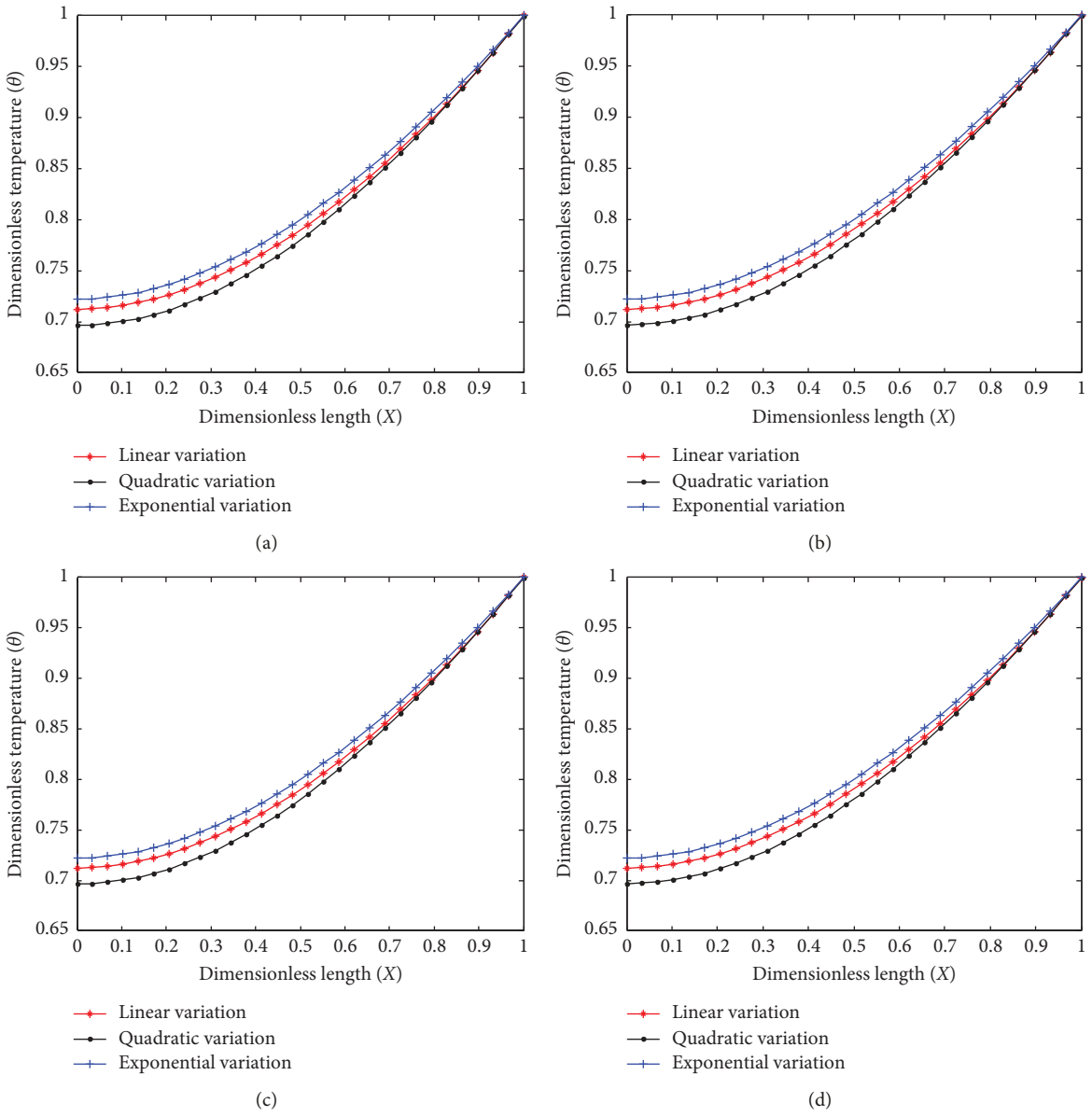

FIGURE 5: Temperature distribution in the fin for different variable thermal conductivity at (a) $\tau = 0.1$, (b) $\tau = 0.15$, (c) $\tau = 0.30$, and (d) $\tau = 0.35$.

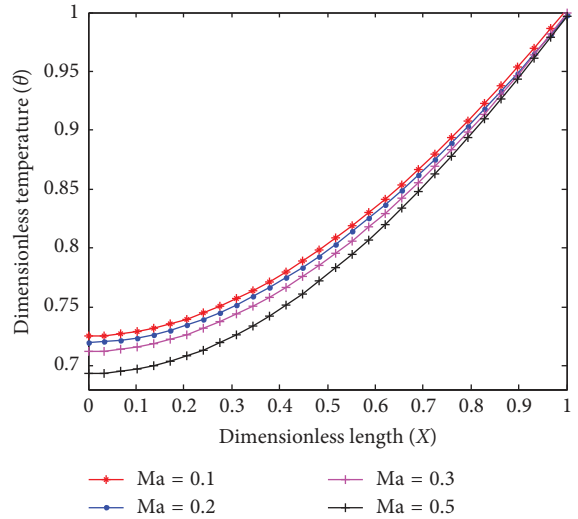

FIGURE 6: Effects of the magnetic field parameter on the temperature distribution.

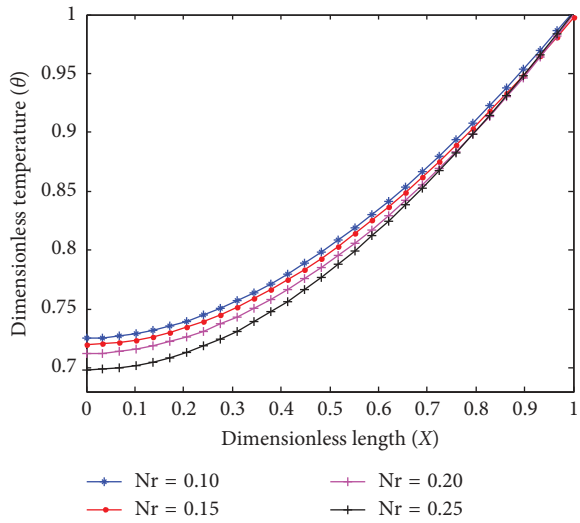

Figure 7: Effects of the radiation number on the temperature distribution.

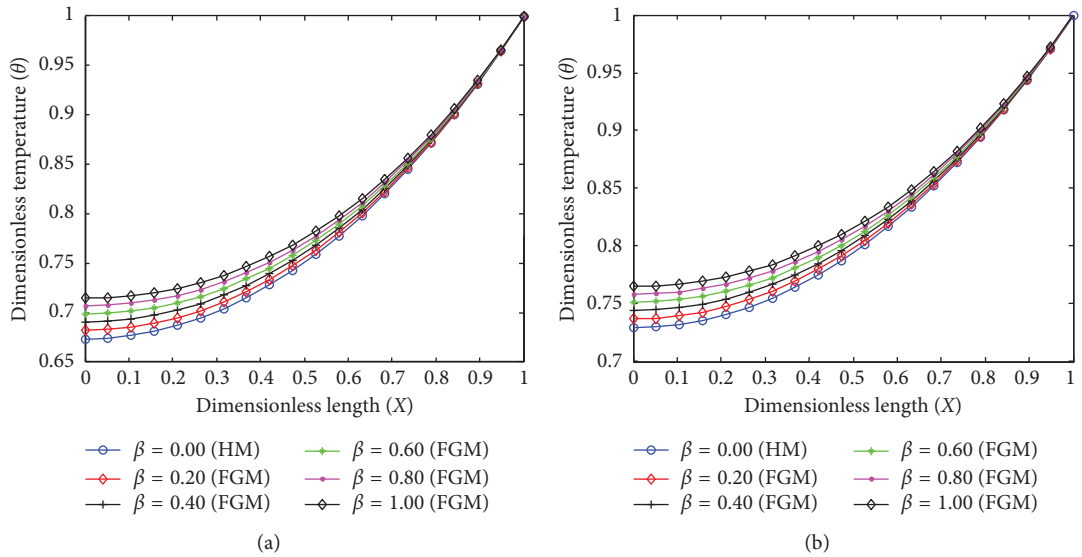

Figure 8: Temperature distribution in the fin for varying thermogeometric parameter under (a) linear-law function and (b) exponential-law functions.

homogeneity index, β, the temperature gradient decreases as shown in the figures. Furthermore, the rate of heat transfer enhancement for FGM longitudinal fin increases by increasing the in-homogeneity index, β, of the FGM fin. It is therefore established from these results that the temperature profiles of the fin are highly sensitive in linear-law function with FGM than that of power-law function. In addition, the application of fin with FGM is favourable at low thermogeometric convective, magnetic field, and radiative parameters since the difference between fin with FGM and fin with HM fin temperature profiles slightly decreases as the dimensionless thermogeometric parameters increase. It could be inferred from the figures that the application of fin with FGM decreases the thermal resistance along the fin, and consequently, a fin with FGM has higher temperature at the fin tip than the fin with HM. The rate of energy saving in power-law class FGM heat sink is significantly higher than the linear class FGM heat sink.

Table 1 shows the comparison of results between the DTM and the exact analytical method. From the table, it is established that the temperature predictions in the heat sink using the differential transformation method are in excellent agreement with the results of the numerical methods.

6. Conclusion

Transient thermal analysis of a convective-radiative fin with functionally graded materials under the influence of magnetic field has been presented in this work. Different variations of thermal conductivity according to linear, quadratic, and exponential variations considered in the

Table 1: Comparison of results when Nc = 0.01, Ma = 0.1, and Nr = 0.5.

X	Exact	DTM	Error
0.00	0.863499158	0.863499231	0.000000073
0.05	0.863828540	0.863828568	0.000000028
0.10	0.864817031	0.864817090	0.000000059
0.15	0.866465671	0.866465743	0.000000072
0.20	0.868776195	0.868776261	0.000000066
0.25	0.871751037	0.871751104	0.000000067
0.30	0.875393336	0.875393404	0.000000068
0.35	0.879706946	0.879707010	0.000000064
0.40	0.884696438	0.884696500	0.000000062
0.45	0.890367120	0.890367181	0.000000061
0.50	0.896725040	0.896725096	0.000000056
0.55	0.903777007	0.903777060	0.000000053
0.60	0.911530606	0.911530658	0.000000052
0.65	0.919994212	0.919994259	0.000000047
0.70	0.929177015	0.929177056	0.000000041
0.75	0.939089039	0.939089079	0.00000004
0.80	0.949741166	0.949741203	0.000000037
0.85	0.961145166	0.961145189	0.000000023
0.90	0.973313722	0.973313764	0.000000042
0.95	0.986260463	0.986260549	0.000000086
1.00	1.000000000	1.000000000	0.000000000

thermal models are solved analytically with the aids of Bessel, Legendre, and modified Bessel functions, respectively. The impacts of Lorentz force and radiative as well as in-homogeneity index on the thermal performance of the fin have been investigated and discussed. The results show that increase in radiative and magnetic field parameters as well as in-homogeneity index improve the thermal performance of the fin. Also, it was established that the transient responses of the functionally graded material (FGM) fin with quadratic-law and exponential-law function show the slowest and fastest thermal responses, respectively. It is therefore hoped that the study will aid in the design and optimization approach of the fin for improved heat transfer enhancements of thermal systems under the influence of magnetic field.

Nomenclature

a_r: Aspect ratio of the porous fin base area to the surface area
A: Cross-sectional area of the fins (m^2)
A_b: Porous fin base area
A_s: Porous fin surface area
Bi: Biot number
h: Heat transfer coefficient ($W{\cdot}m^{-2}{\cdot}k^{-1}$)
h_b: Heat transfer coefficient at the base of the fin ($W{\cdot}m^{-2}{\cdot}k^{-1}$)
c_p: Specific heat of the fluid passing through the porous fin (J/kg·K)
Da: Darcy number
g: Gravity constant (m/s^2)
h: Heat transfer coefficient over the fin surface ($W/m^2{\cdot}K$)
H: Dimensionless heat transfer coefficient at the base of the fin ($W{\cdot}m^{-2}{\cdot}k^{-1}$)
k: Thermal conductivity of the fin material ($W{\cdot}m^{-1}{\cdot}k^{-1}$)
k_b: Thermal conductivity of the fin material at the base of the fin ($W{\cdot}m^{-1}{\cdot}k^{-1}$)
k_{eff}: Effective thermal conductivity ratio
K: Permeability of the porous fin (m^2)
L: Length of the fin (m)
M: Dimensionless thermogeometric parameter
m: Mass flow rate of fluid passing through the porous fin (kg/s)
P: Perimeter of the fin (m)
Q: Dimensionless heat transfer rate per unit area
q_b: Heat transfer rate per unit area at the base (W/m^2)
Q_b: Dimensionless heat transfer rate at the base in the porous fin
Q_s: Dimensionless heat transfer rate at the base in the solid fin
Ra: Rayleigh number
S_h: Porosity parameter
t: Thickness of the fin
T_b: Base temperature (K)
T: Fin temperature (K)
T_a: Ambient temperature (K)
T_b: Temperature at the base of the fin (K)
v: Average velocity of fluid passing through the porous fin (m/s)
x: Axial length measured from the fin tip (m)
X: Dimensionless length of the fin
w: Width of the fin.

Greek Symbols
β: In-homogeity index
δ: Thickness of the fin (m)
δ_b: Fin thickness at its base
γ: Dimensionless internal heat generation parameter
θ: Dimensionless temperature
θ_b: Dimensionless temperature at the base of the fin
η: Efficiency of the fin
β': Coefficient of thermal expansion (K^{-1})
ε: Porosity or void ratio
υ: Kinematic viscosity (m^2/s)
ρ: Density of the fluid (kg/m^3).

Subscripts
s: Solid properties
f: Fluid properties
eff: Effective porous properties.

Data Availability

The data used to support the findings of this study are available from the corresponding author upon request.

Conflicts of Interest

The authors declare that there are no conflicts of interest regarding the publication of this paper.

Acknowledgments

The authors express their sincere appreciation to University of Lagos, Nigeria, for providing material supports and good environment for this work. This research was performed as part of the employment of the authors under the University of Lagos, Nigeria.

References

[1] S. Kiwan and M. A. Al-Nimr, "Using porous fins for heat transfer enhancement," *Journal of Heat Transfer*, vol. 123, no. 4, pp. 790–795, 2000.

[2] S. Kiwan, "Effect of radiative losses on the heat transfer from porous fins," *International Journal of Thermal Sciences*, vol. 46, no. 10, pp. 1046–1055, 2007.

[3] S. Kiwan, "Thermal analysis of natural convection porous fins," *Transport in Porous Media*, vol. 67, no. 1, pp. 17–29, 2006.

[4] S. Kiwan and O. Zeitoun, "Natural convection in a horizontal cylindrical annulus using porous fins," *International Journal of Numerical Methods for Heat & Fluid Flow*, vol. 18, no. 5, pp. 618–634, 2008.

[5] A. Shalchi-Tabrizi and H. R. Seyf, "Analysis of entropy generation and convective heat transfer of Al_2O_3 nanofluid flow in a tangential micro heat sink," *International Journal of Heat and Mass Transfer*, vol. 55, no. 15-16, pp. 4366–4375, 2012.

[6] S. M. H. Hashemi, S. A. Fazeli, H. Zirakzadeh, and M. Ashjaee, "Study of heat transfer enhancement in a nanofluid-cooled miniature heat sink," *International Communications in Heat and Mass Transfer*, vol. 39, no. 6, pp. 877–884, 2012.

[7] T.-C. Hung, W.-M. Yan, X.-D. Wang, and C.-Y. Chang, "Heat transfer enhancement in microchannel heat sinks using nanofluids," *International Journal of Heat and Mass Transfer*, vol. 55, no. 9-10, pp. 2559–2570, 2012.

[8] H. R. Seyf and M. Feizbakhshi, "Computational analysis of nanofluid effects on convective heat transfer enhancement of micro-pin-fin heat sinks," *International Journal of Thermal Sciences*, vol. 58, pp. 168–179, 2012.

[9] S. A. Fazeli, S. M. H. Hashemi, H. Zirakzadeh, and M. Ashjaee, "Experimental and numerical investigation of heat transfer in a miniature heat sink utilizing silica nanofluid," *Superlattices and Microstructures*, vol. 51, no. 2, pp. 247–264, 2012.

[10] S.-M. Kim and I. Mudawar, "Analytical heat diffusion models for different micro-channel heat sink cross-sectional geometries," *International Journal of Heat and Mass Transfer*, vol. 53, no. 19-20, pp. 4002–4016, 2010.

[11] P. Naphon, S. Klangchart, and S. Wongwises, "Numerical investigation on the heat transfer and flow in the mini-fin heat sink for CPU," *International Communications in Heat and Mass Transfer*, vol. 36, no. 8, pp. 834–840, 2009.

[12] P. Naphon and O. Khonseur, "Study on the convective heat transfer and pressure drop in the micro-channel heat sink," *International Communications in Heat and Mass Transfer*, vol. 36, no. 1, pp. 39–44, 2009.

[13] T. Y. Kim and S. J. Kim, "Fluid flow and heat transfer characteristics of cross-cut heat sinks," *International Journal of Heat and Mass Transfer*, vol. 52, no. 23-24, pp. 5358–5370, 2009.

[14] T.-C. Hung, W.-M. Yan, and W.-P. Li, "Analysis of heat transfer characteristics of double-layered microchannel heat sink," *International Journal of Heat and Mass Transfer*, vol. 55, no. 11-12, pp. 3090–3099, 2012.

[15] Z. M. Wan, G. Q. Guo, K. L. Su, Z. K. Tu, and W. Liu, "Experimental analysis of flow and heat transfer in a miniature porous heat sink for high heat flux application," *International Journal of Heat and Mass Transfer*, vol. 55, no. 15-16, pp. 4437–4441, 2012.

[16] D. Lelea, "Effects of inlet geometry on heat transfer and fluid flow of tangential micro-heat sink," *International Journal of Heat and Mass Transfer*, vol. 53, no. 17-18, pp. 3562–3569, 2010.

[17] X. Yu, J. Feng, Q. Feng, and Q. Wang, "Development of a plate-pin fin heat sink and its performance comparisons with a plate fin heat sink," *Applied Thermal Engineering*, vol. 25, no. 2-3, pp. 173–182, 2005.

[18] L. Chai, G. Xia, M. Zhou, and J. Li, "Numerical simulation of fluid flow and heat transfer in a microchannel heat sink with offset fan-shaped reentrant cavities in sidewall," *International Communications in Heat and Mass Transfer*, vol. 38, no. 5, pp. 577–584, 2011.

[19] Wikipedia, "Functionally graded material," https://en.wikipedia.org/wiki/functionally_graded_material.

[20] R. Hassanzadeh and M. Bilgili, "Improvement of thermal efficiency in computer heat sink using functionally graded materials," *Communications on Advanced Computational Science with Applications*, Article ID cacsa-3 pages, 2014.

[21] C. Bilgili, "Thermal management technologies for electronic packaging: current capabilities and future challenges for modelling tools," in *Proceedings of 2008 10th Electronics Packaging Technology Conference*, pp. 527–532, Singapore, December 2008.

[22] D. P. Kulkarni and D. K. Das, "Analytical and numerical studies on microscale heat sinks for electronic applications," *Applied Thermal Engineering*, vol. 25, no. 14-15, pp. 2432–2449, 2005.

[23] T. Dang, J.-T. Teng, and J.-C. Chu, "A study on the simulation and experiment of a microchannel counter-flow heat exchanger," *Applied Thermal Engineering*, vol. 30, no. 14-15, pp. 2163–2172, 2010.

[24] L. Li, M. Nagar, and X. Jie, "Effect of thermal interface materials on manufacturing and reliability of Flip Chip PBGA and SiP packages," in *Proceedings of 2008 58th Electronic Components and Technology Conference*, pp. 973–978, Lake Buena Vista, FL, USA, May 2008.

[25] X. Luo, W. Xiong, T. Cheng, and S. Liu, "Design and optimization of horizontally-located plate fin heat sink for high power LED street lamps," in *Proceedings of 2009 59th Electronic Components and Technology Conference*, pp. 854–859, San Diego, CA, USA, May 2009.

[26] R. Kandasamy, X.-Q. Wang, and A. S. Mujumdar, "Transient cooling of electronics using phase change material (PCM)-based heat sinks," *Applied Thermal Engineering*, vol. 28, no. 8-9, pp. 1047–1057, 2008.

[27] K.-T. Chiang, "Modeling and optimization of designing parameters for a parallel-plain fin heat sink with confined impinging jet using the response surface methodology," *Applied Thermal Engineering*, vol. 27, no. 14-15, pp. 2473–2482, 2007.

[28] D. Gottlieb and S. A. Orszag, *Numerical Analysis of Spectral Methods: Theory and Applications (CBMS-NSF Regional Conference Series in Applied Mathematics)*, Society for Industrial and Applied Mathematics, Philadelphia, PA, USA, 1987.

[29] Y. H. Claudio Canuto, A. Quarteroni, and T. A. Zang, *Spectral Methods in Fluid Dynamics*, Springer Berlin Heidelberg, Berlin, Germany, 1988.

[30] R. Peyret, *Spectral Methods for Incompressible Viscous Flow*, Springer-Verlag, New York, NY, USA, 2002.

[31] F. B. Belgacem and M. Grundmann, "Approximation of the wave and electromagnetic diffusion equations by spectral method," *SIAM Journal on Scientific Computing*, vol. 20, pp. 13–32, 1998.

[32] X. Shan, D. Montgomery, and H. Chen, "Nonlinear magnetohydrodynamics by Galerkin-method computation," *Physical Review A*, vol. 44, no. 10, pp. 6800–6818, 1991.

[33] J. P. Wang, "Fundamental problems in spectral methods and finite spectral method," *Acta Aerodynamica Sinica*, vol. 19, pp. 161–171, 2001.

[34] E. M. E. Elbarbary and M. El-Kady, "Chebyshev finite difference approximation for the boundary value problems," *Applied Mathematics and Computation*, vol. 139, no. 2-3, pp. 513–523, 2003.

[35] Z. J. Huang and Z. J. Zhu, "Chebyshev spectral collocation method for solution of Burgers' equation and laminar natural convection in two-dimensional cavities," B.Sc. thesis, University of Science and Technology of China, Hefei, China, 2009.

[36] N. T. Eldabe and M. E. M. Ouaf, "Chebyshev finite difference method for heat and mass transfer in a hydromagnetic flow of a micropolar fluid past a stretching surface with Ohmic heating and viscous dissipation," *Applied Mathematics and Computation*, vol. 177, no. 2, pp. 561–571, 2006.

[37] A. H. Khater, R. S. Temsah, and M. M. Hassan, "A Chebyshev spectral collocation method for solving Burgers'-type equations," *Journal of Computational and Applied Mathematics*, vol. 222, no. 2, pp. 333–350, 2008.

[38] E. H. Doha, A. H. Bhrawy, and S. S. Ezz-Eldien, "Efficient Chebyshev spectral methods for solving multi-term fractional orders differential equations," *Applied Mathematical Modelling*, vol. 35, no. 12, pp. 5662–5672, 2011.

[39] B. Kundu, R. Das, P. A. Wankhade, and K.-S. Lee, "Heat transfer improvement of a wet fin under transient response with a unique design arrangement aspect," *International Journal of Heat and Mass Transfer*, vol. 127, pp. 1239–1251, 2018.

[40] P. A. Wankhade, B. Kundu, and R. Das, "Establishment of non-Fourier heat conduction model for an accurate transient thermal response in wet fins," *International Journal of Heat and Mass Transfer*, vol. 126, pp. 911–923, 2018.

[41] R. Das and B. Kundu, "Direct and inverse approaches for analysis and optimization of fins under sensible and latent heat load," *International Journal of Heat and Mass Transfer*, vol. 124, pp. 331–343, 2018.

[42] R. Das and B. Kundu, "Estimation of internal heat generation in a fin involving all modes of heat transfer using golden section search method," *Heat Transfer Engineering*, vol. 39, no. 1, pp. 58–71, 2017.

[43] R. Das and B. Kundu, "Prediction of heat generation in a porous fin from surface temperature," *Journal of Thermophysics and Heat Transfer*, vol. 31, no. 4, pp. 781–790, 2017.

[44] S. S. Ezz-Eldien, "New quadrature approach based on operational matrix for solving a class of fractional variational problems," *Journal of Computational Physics*, vol. 317, pp. 362–381, 2016.

[45] A. H. Bhrawy and S. S. Ezz-Eldien, "A new Legendre operational technique for delay fractional optimal control problems," *Calcolo*, vol. 53, no. 4, pp. 521–543, 2015.

[46] S. S. Ezz-Eldien and E. H. Doha, "Fast and precise spectral method for solving pantograph type Volterra integro-differential equations," *Numerical Algorithms*, pp. 1–21, 2018, In press.

[47] A. H. Bhrawy, S. S. Ezz-Eldien, E. H. Doha, M. A. Abdelkawy, and D. Baleanu, "Solving fractional optimal control problems within a Chebyshev-Legendre operational technique," *International Journal of Control*, vol. 90, no. 6, pp. 1230–1244, 2017.

[48] M. G. Sobamowo, "Nonlinear thermal and flow-induced vibration analysis of fluid-conveying carbon Nanotube resting on Winkler and Pasternak foundations," *Thermal Science and Engineering Progress*, vol. 4, pp. 133–149, 2017.

[49] M. G. Sobamowo, O. Adeleye, and A. A. Yinusa, "Analysis of convective-radiative porous fin with temperature-dependent internal heat Generation and magnetic field using Homotopy Perturbation method," *Journal of Computational and Applied Mechanics*, vol. 12, no. 2, pp. 127–145, 2017.

[50] S. T. Lee, M. C. H. Chien, and W. E. Culham, "Vertical single-well pulse testing of a three-layer stratified reservoir," in *Proceedings of SPE Annual Technical Conference and Exhibition*, Society of Petroleum Engineers, Houston, TX, USA, 1984.